Neuromuscular synaptic function in mice lacking major subsets of gangliosides

Femke M.P. Zitman[a,b], Boyan Todorov[c], Bart C. Jacobs[d], Jan J. Verschuuren[a], Keiko Furukawa[e], Koichi Furukawa[e], Hugh J. Willison[f], Jaap J. Plomp[a,b].

Departments of [a]Neurology and [b]Molecular Cell Biology – Group Neurophysiology, and [c]Human Genetics, Leiden University Medical Centre, PO Box 9600, NL-2300 RC Leiden, The Netherlands.
[d]Departments of Neurology and Immunology, Erasmus MC, 's-Gravendijkwal 230, 3015 CE Rotterdam, The Netherlands.
[e]Department of Biochemistry II, Nagoya University Graduate School of Medicine, Nagoya, Japan
[f]Divison of Clinical Neurosciences, Glasgow Biomedical Research Centre, University of Glasgow, Glasgow G12 8TA, UK.

Address for correspondence:
Dr. J.J. Plomp, PhD
Leiden University Medical Centre
MCB-Neurophysiology
Research Building, S5P, room T-05-032
P.O. Box 9600, 2300 RC Leiden
The Netherlands
Phone +31 71 526 9768
E-mail j.j.plomp@lumc.nl

Running title: Role of gangliosides in synaptic function

Abbreviations: ACh, acetylcholine; dKO, double knockout (β1,4-GalNAc-transferase and α2,8-sialyltransferase knockout); EPP, endplate potential; GalNAc, *N*-acetyl galactosamine; GBS, Guillain-Barré syndrome; GD3s-KO, α2,8-sialyltransferase knockout; GM2s-KO, β1,4-GalNAc-transferase knockout; MEPP, miniature endplate potential; MFS, Miller Fisher syndrome; NeuAc, neuraminic acid; NMJ, neuromuscular junction; WT, wildtype.

Abstract

Gangliosides are a family of sialylated glycosphingolipids enriched in the outer leaflet of cell neuronal membranes, in particular at synapses. Therefore, they have been hypothesized to play a functional role in synaptic transmission. We have measured in detail the electrophysiological parameters of synaptic transmission at the neuromuscular junction (NMJ) *ex vivo* of a GD3-synthase knockout mouse, expressing only the O- and a-series gangliosides, as well as of a GM2/GD2-synthase*GD3-synthase double-knockout (dKO) mouse, lacking all gangliosides except GM3. No major synaptic deficits were found in either *null*-mutant. However, some extra degree of rundown of acetylcholine release at high intensity use was present at the dKO NMJ and a temperature-specific increase in acetylcholine release at 35 °C was observed in GD3-synthase knockout NMJs, compared to wildtype. These results indicate that synaptic transmission at the NMJ is not crucially dependent on the particular presence of most ganglioside family members and remains largely intact in the sole presence of GM3 ganglioside. Rather, presynaptic gangliosides appear to play a modulating role in temperature- and use-dependent fine-tuning of transmitter output.

Introduction

Neuronal membranes contain high levels of gangliosides (Ledeen, 1985), which are a diverse family of sialylated glycosphingolipids (Fig. 1; Svennerholm, 1994; Ngamukote et al., 2007). *Complex* gangliosides GM1, GD1a, GD1b and GT1b are the major species in central and peripheral nervous tissue (Tettamanti et al., 1973; Gong et al., 2002). *Simple* gangliosides (e.g. GM3 and GD3) are relatively abundant in early embryonic brain but decrease rapidly in later stages (Ngamukote et al., 2007).

Gangliosides are components of membrane lipid rafts and are thought to play roles in modulation of membrane-bound enzymes, ion-channel kinetics, cell-adhesion, neuritogenesis, cell-signaling and membrane stability and maintenance (Yates and Rampersaud, 1998; Hakomori, 2003; Hashiramoto et al., 2006; Sohn et al., 2006; Ledeen and Wu, 2006; Sonnino et al., 2007; Susuki et al., 2007; Wu et al., 2007).

Importantly, gangliosides are involved in neurological disease. Anti-ganglioside antibodies have been shown in the Guillain-Barré syndrome (GBS), where anti-GM1 antibodies are mainly associated with motor variants of the disease and anti-GQ1b antibodies with the Miller Fisher syndrome (MFS) variant (Willison and Yuki, 2002; Ang et al., 2004). Ganglioside metabolism is disturbed in an infantile epilepsy syndrome (Simpson et al., 2004), in Sandhoff's disease (Liu et al., 1999), and possibly in Huntington's disease (Desplats et al., 2007) and multiple sclerosis (Marconi et al., 2006). Gangliosides can also function as cell surface receptors for microbial toxins (Fishman, 1982; Bullens et al., 2002). Experimental studies in mice by us and others have shown that GBS/MFS-associated anti-ganglioside antibodies can mediate functional and structural damage to neuromuscular junctions (NMJs) (Buchwald et al., 1995; Plomp et al., 1999; Ortiz et al., 2001; O'Hanlon et al., 2001; Halstead et al., 2004; Santafe et al., 2005).

Gangliosides contain negatively charged sialic acid residues that contribute to the surface charge of membranes and thereby potentially modulate H^+ and Ca^{2+} homeostasis as well as voltage-gated ion-channel functioning. In addition, they influence membrane viscosity in a temperature-dependent way and thereby indirectly modulate ion-channel activities (Kappel et al., 2000). Gangliosides in the vicinity of ion-channels or -pumps may directly influence their kinetics and function (Wang et al., 1999; Ledeen and Wu, 2006). Furthermore, they may influence intracellular Ca^{2+} homeostasis (Wu et al., 2005). Recent functional studies using anti-ganglisode antibodies suggest a relationship between gangliosides and voltage-gated Ca^{2+} channels (Ortiz et al., 2001; Santafe et al., 2005; Nakatani et al., 2007).

In the light of their known effects on ion-channels and their particular abundance in synaptic regions, gangliosides are thought to play a role in neurotransmitter release, which is critically dependent on presynaptic ion-channel function (Wieraszko and Seifert, 1985; Ramirez et al., 1990; Egorushkina et al., 1993; Takamiya et al., 1996; Tanaka et al., 1997; Furuse et al., 1998; Ando et al., 1998; Meir et al., 1999; Chiavegatto et al., 2000; Bullens et al., 2002; Hakomori, 2003; Proia, 2003). Several important proteins of the release machinery co-localize with gangliosides within lipid rafts (Chamberlain et al., 2001; Lang et al., 2001; Taverna et al., 2004; Salaun et al., 2004).

β1,4-GalNAc-transferase (or GM2/GD2-synthase, EC 2.4.1.92) knockout (GM2s-KO) mice lack complex gangliosides (Fig. 1; Takamiya et al., 1996; Sheikh et al., 1999) and develop sensory and motor coordination defects upon aging (Chiavegatto et al., 2000; Sugiura et al., 2005). Previously we investigated synaptic transmission in young GM2s-KO mice at NMJs *ex vivo* (Bullens et al., 2002). Surprisingly, we found that complex gangliosides were redundant for acetylcholine (ACh) release at room temperature. However, reduced release was found at 17 °C, suggesting that complex gangliosides are involved in temperature-stabilization of synaptic transmission.

Two additional ganglioside-deficient mice have been generated: 1) a GD3-synthase knockout (GD3s-KO) mouse (Okada et al., 2002), which lacks the gene coding for α2,8-sialyltransferase (EC 2.4.99.8) and only expresses the O- and a-series gangliosides and 2) a GM2s*GD3s double knockout (dKO) mouse (Kawai et al., 2001; Inoue et al., 2002), which lacks the genes coding for both β1,4-GalNAc-transferase and α2,8-sialyltransferase, thereby only expressing GM3 ganglioside (Fig. 1). GD3s-KO mice are viable and fertile and show no overt phenotype, while dKO mice display sudden death starting from about 7-12 weeks of age. Here, we studied the roles of specific ganglioside subsets in neurotransmission by characterizing neuromuscular function in these two *null*-mutants.

Material and methods

Mice

We used male and female GD3s-KO mice (Okada et al., 2002) for experiments. To generate the dKO mice, homozygous female GM2s-KO mice (Takamiya et al., 1996) were crossbred with male homozygous GD3s-KO mice. Their double heterozygous progeny was then intercrossed to generate homozygous dKO mice. Genotyping was performed as described (Takamiya et al., 1996; Inoue et al., 2002). Male and female dKO mice were used in the experiments. Wildtype (WT) mice were used as controls. The mice were 6-13 weeks of age. Body weights of WT, GD3s-KO and dKO mice used were 20.3 ± 1.0, 21.1 ± 0.8 and 21.5 ± 0.8 g, respectively. All animal experiments were carried out according to Dutch law and Leiden University guidelines.

In vivo neuromuscular function tests

The inverted screen hanging test was used to assess fatigability of limb muscles as described before (Kaja et al., 2007). The test ended upon falling or completing the maximum hanging time which was set at 300 s.

Muscle strength was assessed using a grip strength meter (type 303500, Technical and Scientific Equipment GmbH, Bad Homburg, Germany) and essentially performed as described (Kaja et al., 2007). As grip strength the peak force value was taken of a pull measured by the grip-strength-meter. Each trial consisted of at least 10 pullings and the averaged value was used for statistical analysis. Values were normalized to the body weights of mice.

Respiratory rate and volume were assessed with non-invasive whole-body plethysmography (RM-80, Columbus Instruments, Ohio, USA). The signal was digitized using a Digidata 1440A interface (Axon Instruments/Molecular Devices, Union City, CA, USA) and analyzed with the event detection feature of Clampfit 9.2 (Axon Instruments/Molecular Devices).

In vitro electrophysiology at the NMJ

Mice were killed by CO_2 asphyxiation. Left and right hemi-diaphragms were dissected with their phrenic nerve attached and mounted in standard Ringer's medium (119 mM NaCl, 4.5 mM KCl, 2 mM $CaCl_2$, 1 mM $MgSO_4$, 1 mM NaH_2PO_4, 23 mM $NaHCO_3$, 11 mM glucose, pH 7.4) at room temperature, pre-gassed with 95% O_2 / 5% CO_2.

Intracellular recordings of miniature endplate potentials (MEPPs) and endplate potentials (EPPs) in the NMJ were made using a glass micro-electrode (10-20 MΩ, filled with 3 M KCl) connected to a Geneclamp 500B (Axon Instruments/Molecular devices) for amplifying and filtering (10 kHz low-pass) of the signal. The signal was digitized using a Digidata 1322A interface (Axon Instruments/Molecular Devices) and analyzed using Clampfit 9.2 (Axon Instruments/Molecular Devices) and Mini Analysis 6.0.3 (Synaptosoft, Fort Lee, USA). Muscle action potentials were eliminated by using the selectively skeletal muscle Na^+ channel blocker, μ-Conotoxin GIIIB (3 μM) (Scientific Marketing Associates, Barnet, Herts, UK). To record EPPs, the phrenic nerve was stimulated at multiple frequencies using a bipolar platinum electrode. The mean EPP and MEPP amplitudes at each NMJ were normalized to -75 mV, with the reversal potential for ACh-induced current assumed to be 0 mV (Magleby and Stevens, 1972). In order to calculate the quantal content for each NMJ, the mean amplitude of the 30 EPPs recorded at low rate (0.3 Hz) stimulation were corrected for non-linear summation (McLachlan and Martin, 1980) and the normalized and corrected mean EPP amplitude was divided by the normalized mean MEPP amplitude (calculated from at least 40 MEPPs sampled). The quantal content is the number of ACh quanta that is released upon a single nerve impulse.

MEPPs were also recorded after addition of hypertonic medium (0.5 M sucrose Ringer's medium), in order to estimate the pool of ACh vesicles ready for immediate release (Stevens and Tsujimoto, 1995; Varoqueaux et al., 2005). In some experiments we tested the effect on EPPs and MEPPs of 200 nM of the $Ca_v2.1$ Ca^{2+} channel blocker ω-agatoxin-IVA (Scientific Marketing Associates) and 10 μM of the Ca_v1 blocker nifedipine (Sigma-Aldrich, Zwijndrecht, The Netherlands).

Temperature of the bath medium was controlled using a Peltier device placed around the recording bath and adjusted by varying the DC output of a power supply (Delta Elektronika, Zierikzee, The Netherlands). A miniature probe connected to a digital thermometer was used to monitor the temperature. Bath temperature was held at 24-26 °C, unless stated otherwise.

Electrophysiological data is presented as group mean ± SEM of the mean muscle values calculated from the mean NMJ values. At least 10 NMJs were sampled per muscle per experimental condition.

Statistical analysis

Statistical differences between groups means were analyzed with an unpaired Student's *t*-test or an analysis of variance (ANOVA), with Bonferroni post-hoc testing, wherever appropriate.

Results

In vivo neuromuscular tests

Neuromuscular synapse dysfunction may lead to respiration difficulties that are detectable in whole body plethysmography (Halstead et al., 2008a). Upon such assessment we found in both the GD3s-KO and dKO mice a lower respiration rate than in WT mice (WT 424 ± 20; GD3s-KO 298 ± 10; dKO 307 ± 14 min^{-1}; n=8-20 mice, $p<0.01$; Fig. 2A, C). The positive peak amplitude of the measured signal, reflecting tidal volume, was ~35% increased in dKO mice (WT 12.2 ± 0.7; GD3s-KO 12.2 ± 0.4; dKO 16.4 ± 0.6 mV; $p<0.01$; Fig. 2B, C). When the signals were normalized to body weight this difference became somewhat smaller but remained statistically significant (WT 0.65 ± 0.03; GD3s-KO 0.59 ± 0.02; dKO 0.77 ± 0.03 mV per g body weight; $p<0.01$ dKO vs. GD3 and $p<0.05$ dKO vs. WT). Fig. 2C shows typical examples of respiration traces recorded.

GD3s-KO mice showed no overt neuromuscular phenotype. In 6 of the 14 dKO mice used, however, we observed symptoms of weakness and/or uncoordinated movement (especially of hind legs). Although grip strength testing indicated normal muscle strength in dKO mice (~6 g/g body weight for each strain; $p=0.30$, n=7-20 mice; Fig. 2D), they performed worse on the inverted mesh (hanging times: WT 300 ± 0; GD3-KO 277 ± 16; dKO 178 ± 28 s; $p<0.05$, n=5-20 mice; Fig. 2E). Symptomatic dKO mice had shorter ($p<0.05$) hanging times (111 ± 39 s) than non-symptomatic dKO mice (228 ± 30 s), but did not differ from each other with respect to the other *in vivo* tests.

Normal basic synaptic electrophysiology in GD3s-KO and dKO mice

Spontaneous uniquantal transmitter release was measured at the diaphragm NMJ. No statistically significant differences were found between genotype groups in MEPP amplitude (~0.9 mV; $p=0.43$, Fig. 3A, E) and MEPP frequency (~1.3 s^{-1}; $p=0.10$, Fig. 3B). The 0.3 Hz nerve stimulation-evoked transmitter release resulted in equal EPP amplitudes for the three groups (~25 mV; $p=0.45$, Fig. 3C, F). The delay between nerve stimulus and start of the EPP was somewhat longer in dKO preparations (WT 1.74 ± 0.09; GD3s-KO 1.84 ± 0.05; dKO 2.16 ± 0.11 ms; $p<0.05$ dKO vs. WT). Quantal content was calculated and appeared not statistically significantly different between groups although there was a tendency towards reduction in the dKO NMJ (WT 47.0 ± 2.7; GD3s-KO 46.1 ± 1.9; dKO 40.3 ± 1.0; $p=0.27$, Fig. 3D). ACh release at the NMJ is almost completely mediated by Ca^{2+} flux through $Ca_v2.1$ (P/Q-type) channels. We probed for compensatory contribution of non-$Ca_v2.1$ channels by

determining the effect of 200 nM ω-agatoxin-IVA ($Ca_v2.1$ blocker) and 10 μM nifedipine (Ca_v1 blocker) on 0.3 Hz evoked ACh release at both dKO and GD3s-KO NMJs. ω-Agatoxin readily reduced the quantal content by 95% at NMJs of both genotypes (from 28.4 ± 1.6 to 1.4 ± 0.3 in the dKO and from 44.1 ± 4.8 to 2.1 ± 0.5 in the GD3s-KO; one hemidiaphragm preparation each, 10-15 NMJs sampled per condition), indicating an almost complete dependence on $Ca_v2.1$, and identical to the reductions we observe routinely at wild-type NMJs (Kaja et al., 2007). This seems to rule out any compensatory contribution by other types of Ca_v channels. The Ca_v1 (L-type) channel blocker nifedipine was without effect on the quantal content measured at dKO and GD3s-KO NMJs, excluding compensation by Ca_v1 channels. The quantal content values were 29.9 ± 2.6 before and 31.3 ± 0.3 after nifedipine in the dKO and 44.1 ± 4.8 before and 44.1 ± 4.1 after nifedipine in the GD3s-KO (one hemidiaphragm preparation each, 10-15 NMJs sampled per condition).

No change in hypertonic shock-induced ACh release

Hypertonic medium (0.5 M sucrose Ringer's) elevated MEPP frequencies to equal levels in the three genotype groups (~48 s^{-1}; p=0.48, n=3-6; Fig. 4). These results suggest an unchanged size of the readily releasable ACh vesicle pool at the NMJ of the two *null*-mutant mice.

More pronounced ACh release rundown at dKO NMJs at high rate nerve stimulation

Some effects of ganglioside composition on transmitter release may only come about at high intensity use of the synapse, stressing the exocytotic molecular machinery. We, therefore, measured EPPs during 1 s high-rate (40 Hz) nerve stimulation trains, which is the approximate physiological firing frequency. At dKO NMJs a modest but statistically highly significant increase in EPP rundown was observed, compared to the other two groups. The EPP rundown plateau levels (the mean of the 21^{st}-35^{th} EPP, expressed as percentage of the first EPP in the train) were: WT 81.2 ± 0.9; GD3s-KO 83.0 ± 0.8; dKO 75.7 ± 0.8% ($p<0.01$, n=11-12 mice; Fig. 5A). At 3 Hz no such difference was encountered. The rundown level in all groups was ~83% (p=0.15). In a separate experimental series on dKO NMJs we explored the behaviour of ACh release at stimulation frequencies of 3, 30, 40, 50, and 70 Hz. Except for 3 Hz (p=0.65), dKO EPPs ran down to a 5-7% lower level than WT at all stimulation frequencies ($p<0.01$; Fig. 5B). Examples of typical EPP rundown traces are shown in Fig. 5C.

Temperature-dependent changes in transmitter release parameters

We explored a possible temperature-dependent functioning of gangliosides by performing synaptic electrophysiological measurements at 17, 20, 30, and 35 °C in a separate series of experiments (Fig. 6). No major differences between GD3s-KO, dKO and WT NMJs in the temperature-dependency of synaptic transmission parameters (MEPP amplitude and frequency, EPP amplitude and quantal content) were observed within this temperature range, other than a somewhat increased MEPP amplitude at GD3s-KO NMJs at 17 °C (~30%, $p<0.05$; Fig. 6A) and an increase of quantal content in GD3s-KO NMJs (~40%, $p<0.05$), compared to WT, at 35 °C (Fig. 6D). The rundown of EPPs at 40 Hz stimulation at dKO NMJs was more pronounced than in GD3s-KO and WT, over the whole temperature range, although only statistically significantly at 25 °C (as described above), 30 and 35 °C test temperatures ($p<0.05$; Fig. 6E). Because the extent of this extra EPP rundown was similar (~25%) at the several temperatures, it can be concluded that the three genotype groups show a similar temperature-dependency for this parameter. The 3 Hz EPP rundown at both dKO and GD3s-KO NMJs was not statistically significantly different from WT at all tested temperatures, although there was a tendency of increased rundown at dKO NMJs. At 17 and 30 °C, 3 Hz EPP rundown at dKO NMJs was somewhat more pronounced than at GD3s-KO NMJs ($p<0.05$; Fig. 6F).

Influence of external Ca^{2+} concentrations on transmitter release

Besides our basic measurements in 2 mM extracellular Ca^{2+}, low (0.2 mM) as well as high (5 mM) Ca^{2+} extracellular medium was applied to explore the Ca^{2+}-dependency of synaptic transmission in the GD3s-KO and dKO mice. MEPP amplitude was ~0.83 mV for each strain at each Ca^{2+} concentration (Fig. 7A). MEPP frequency (Fig. 7B), EPP amplitude (Fig. 7C) and quantal content (Fig. 7D) in WT NMJs were, as expected, steeply dependent on Ca^{2+}. However, we observed no different values of these parameters at GD3s-KO and dKO NMJs, compared to WT, at all Ca^{2+} concentrations, showing unaltered Ca^{2+}-sensitivity of these parameters. As observed at 2 mM Ca^{2+}, the 40 Hz EPP rundown level at dKO NMJs in the presence of 5 mM Ca^{2+} (71.3%) was lower than that in WT (79.8%) and GD3s-KO (78.4%) (Fig. 7E; $p<0.01$). At low Ca^{2+} and 40 Hz stimulation, WT EPPs were potentiated to a plateau level of ~150% of the first EPP. GD3s-KO and dKO NMJs showed similar EPP potentiation ($p=0.83$, Fig. 7E). Example traces of the EPP profiles at 40 Hz stimulation at 0.2 mM Ca^{2+} are shown in Fig. 7F. EPPs at dKO NMJs at 3 Hz stimulation at 5 mM Ca^{2+}, but not at 0.2

and 2 mM, showed a slightly lower EPP rundown level (79.5%) than at WT (84.8%) and GD3s-KO (85.1%) NMJs (Fig. 7G, $p<0.01$). We assessed 25 ms paired-pulse facilitation by comparing the first and second EPP of 40 Hz trains, but found no statistically significant differences between GD3s-KO, dKO and WT NMJs at any of the Ca^{2+} concentrations tested (Fig. 7H).

Discussion

We studied the effects of changed ganglioside profiles in neuronal membranes on synaptic transmission by characterizing NMJ function in GD3s-KO mice, lacking b- and c-series gangliosides, and in dKO mice, lacking all ganglioside types except GM3 (Fig. 1). However, we found no major synaptic deficits in both *null*-mutants. This is quite surprising, in view of studies suggesting a synaptic role for gangliosides on the basis of exogenous ganglioside application (Tanaka et al., 1997; Ando et al., 1998), as well as the reported co-localization in lipid rafts of gangliosides and proteins important for neuroexocytosis (Chamberlain et al., 2001; Lang et al., 2001; Taverna et al., 2004; Salaun et al., 2004). The only changes we observed were some extra degree of rundown of transmitter release at high intensity use at the dKO NMJ and a temperature-specific increase in quantal content at 35 °C in GD3s-KO NMJs, compared to WT. These results indicate that synaptic transmission at the NMJ is not crucially dependent on any particular ganglioside and remains largely intact in the sole presence of GM3 ganglioside.

In vivo neuromuscular analysis

We have performed some orienting *in vivo* characterization of neuromuscular function of the GD3s-KO and dKO mice. Previously we showed that severe paralysis of mouse diaphragm muscle leads to reduced respiration rate and tidal volume in whole body plethysmography (Halstead et al., 2008b). Although we here observed some reduction in respiration rate in both GD3s-KO and dKO mice, tidal volume was not reduced (in fact, there was ~35% increase in the dKO), making severe diaphragm paralysis highly unlikely. Therefore, these changes in respiration patterns probably have a central (possibly synaptic) origin. The reduced hanging time of dKO mice in the inverted mesh test is at least not due to initial forelimb muscle weakness because grip strength testing appeared normal. Although most likely due to central dysfunction, it can not be excluded that the reduced inverted mesh performance has a fatigue component due to increased rundown of transmitter release at the NMJ (see below).

Basic synaptic transmission

In standard physiological medium at 25 °C the variations in ganglioside composition at GD3s-KO and dKO NMJs did not seriously limit synaptic function. The rate of uniquantal ACh release, measured as MEPP frequency, was not different from the WT control NMJs.

Uniquantal size, measured as MEPP amplitude, as well as the amount of ACh released upon 0.3 Hz nerve stimulation were similar in the three genotypes. These unchanged synaptic function parameters at GD3s-KO and dKO NMJs show that at 0.3 Hz stimulation there is a normal invasion of the nerve impulse into the presynaptic nerve ending and a normal translation of this depolarization into transmitter release. Apparently, the function of voltage-gated Na^+, K^+ and Ca^{2+} channels involved in these processes is not impeded by either the loss of b- and c-series gangliosides or by the loss of all gangliosides except GM3. Some degree of ion-channel dysfunction may be present in the dKO phrenic nerve, because we observed ~25% longer delay between nerve stimulus and postsynaptic response in dKO preparations, compared to WT. Although we have not investigated whether this effect is either due to extra synaptic delay or to slower axonal action potential conduction, the observation that GM1 and GD1a are necessary for stability and ion-channel composition of motor nerve nodes of Ranvier (Susuki et al., 2007) favors the latter possibility. Our experiments with specific $Ca_v2.1$ and Ca_v1 Ca^{2+} channel blockers indicated no compensatory contribution by non-$Ca_v2.1$ Ca^{2+} channels to ACh release at both dKO and GD3s-KO NMJs.

Previously we demonstrated a redundancy for the set of complex gangliosides (i.e. the gangliosides from all series with more than two non-sialic acid sugar residues; Fig. 1) by finding unaltered basic synaptic function at NMJs of GM2s-KO mice (Bullens et al., 2002). Our present results in dKO and GD3s-KO mice, in combination with this previous study, show that the sole presence of GM3 ganglioside is sufficient to support neurotransmitter release at the NMJ. GM3 is upregulated in dKO whole brains (Kawai et al., 2001) and such an accummulation may also take place at the presynaptic motoneuronal membrane, possibly enhancing compensatory effects of GM3 in supporting neurotransmitter release upon absence of all other types of gangliosides. Alternatively, gangliosides might not influence the function of ion-channels and/or other membrane factors at mouse presynaptic nerve terminal at all. In other organisms, like *Drosophila melanogaster,* functional synapses exist in spite of the inability to produce gangliosides (Roth et al., 1992; Chen et al., 2007). This shows that gangliosides are not a general prerequisite for synaptic function. However, such absence of a biological role for gangliosides in mammals is rather unlikely in view of the presence of such a highly organized ganglioside synthesis system and, furthermore, the demonstrated severe neurodegeneration in transgenic mice lacking all gangliosides *including* GM3 (Yamashita et al., 2005) and the severe neurological symptoms in human babies with loss-of-function mutated GM3-synthase (Simpson et al., 2004). Therefore, it would be of interest to investigate synaptic transmission in GM3-synthase *null*-mutant mice.

Increased rundown of high-rate transmitter release at dKO synapses

We observed a more pronounced rundown of high rate (30-70 Hz) nerve stimulation-evoked ACh release at dKO NMJs (EPP rundown plateau levels, expressed as percentage of the first EPP in the trains, were ~6% lower than WT). In contrast, GD3s-KO NMJs showed a 40 Hz rundown level comparable to the WT control. This more pronounced rundown of ACh release at dKO NMJs is, however, not to be expected to negatively impact on successful synaptic transmission. From the mean dKO EPP amplitude of 24 mV and the published safety factor for the mouse NMJ of at least 2.4 (Wood and Slater, 2001) it can be calculated that EPPs of more than 10 mV will result in successful transmission. Even at maximal rundown (to a plateau level of ~66% of their initial value, at 70 Hz stimulation), dKO EPPs would remain ~16 mV, i.e. large enough to trigger an action potential in the muscle fibre. This could explain the absence of overt muscle weakness in the dKO mice. However, it can not be excluded that a more pronounced EPP rundown underlies the worse performance of dKO mice on the inverted mesh, which tests for fatigue on the longer duration scale (minutes). It may be that the extra EPP rundown in dKO mice became more prominent upon such long-duration and high-intensity use, resulting in subthreshold EPPs.

Rundown of neurotransmitter release is presumably depending on a combination of the inactivation characteristics of presynaptic Ca^{2+} channels and the size and replenishment rate of the pool of releasable ACh vesicles. At least the pool size in dKO motor nerve terminals seems not reduced because MEPP frequency after addition of hypertonic medium, being a measure for pool size (Stevens and Tsujimoto, 1995; Varoqueaux et al., 2005), was not reduced compared to WT. The extra EPP rundown at dKO NMJs was found at most temperatures and Ca^{2+} concentrations tested here. Previously, we analyzed synaptic function at NMJs of GM2s-KO mice and found some extra rundown of EPP amplitude during high frequency stimulation in particular at 30-35°C and at a high extracellular Ca^{2+} concentration (Bullens et al., 2002). However, GD3s-KO NMJs did not show extra EPP rundown at any condition. This suggests a role for the O- and/or a-series gangliosides in transmitter release at high frequency nerve stimulation, which could be supported by the finding that in particular GM1 ganglioside influences cellular Ca^{2+} membrane flux and homeostasis (Wu et al., 2004), including stimulation of Ca^{2+} influx in some cell types (Wu et al., 1990). If GM1 would promote Ca^{2+} influx at the motor nerve terminal through slowing down Ca^{2+} channel inactivation this could explain the extra EPP rundown in the dKO NMJs where GM1 is

absent. Ion-channel kinetics have been shown to be influenced by gangliosides, either through an electrical effect of the negative charges on their head groups or by an indirect mechanical effect through their ability to control membrane fluidity (Kappel et al., 2000).

Temperature-dependency

Gangliosides have been hypothesized to play a role in thermal stabilization of the neuronal membrane, including adaptation of ion-channel function (Rahmann et al., 1998). We observed a slight tendency of the quantal content at dKO and GD3s-KO NMJs to increase with increasing temperature. At 35 °C this resulted in statistically significantly higher level (~40%) at GD3s-KO NMJs, compared to the WT level which itself remained more or less equal at all temperatures tested. On the basis of this observation it can be hypothesized that gangliosides inhibit transmitter release, e.g. through a (temperature-dependent) effect on activation and/or inactivation of presynaptic voltage-dependent K^+ and/or Ca^{2+} channels. The negative charges on extracellular sialic acid residues of gangliosides contribute to membrane surface charge and may thus influence voltage-dependent properties of ion-channels (Green and Andersen, 1991). For instance, it has recently been shown that removal of sialic acid from the extracellular neuronal membrane by neuraminidase treatment shifts the activation- and inactivation-voltage of Na^+ channels (Isaev et al., 2007), although it remains unclear whether removal of sialic acid from either the surrounding gangliosides or the ion-channel protein itself is causing this effect. The tendency for increased quantal content at 35 °C at dKO compared to WT NMJs indicates that the presence of GM3 alone is not sufficient to keep quantal content at WT level. This may be related to the relatively low level of sialylation of GM3 (only a single sialic acid residue) as compared to other types of gangliosides, because this degree influences the specific effects of gangliosides on ion-channel function (Kappel et al., 2000). An alternative explanation for the tendency of an increase of quantal content at GD3s-KO and dKO NMJs at the higher temperatures tested could be an increased Ca^{2+} availability. Gangliosides have temperature-dependent Ca^{2+} binding sites of which the amount is positively associated with the extent of sialylation (Rahmann et al., 1998). Therefore, loss of sialic acid density in the vicinity of presynaptic voltage-gated Ca^{2+} channels could lead to less adequate Ca^{2+} buffering and thus to increased ACh release. Such an effect seems to occur rather specifically at temperatures around 35 °C, because in our Ca^{2+} variation experiments at 25 °C all GD3s and dKO synaptic parameters except dKO EPP rundown showed normal Ca^{2+}-dependencies.

In conclusion, our results show that most types of gangliosides are not crucially important for synaptic transmission at the mouse NMJ but, rather, have a role in temperature- and use-dependent fine-tuning of transmitter release level. It remains to be directly shown whether the remaining (and possibly upregulated) presence of the simple ganglioside GM3 at dKO membranes explains the partial redundancy of all other gangliosides in neurotransmission.

Acknowledgements

This work was sponsored by grants from the Prinses Beatrix Fonds (#MAR04-0213) and from the Wellcome Trust (060349, 077041). We thank Marloe Pijnacker for excellent caretaking of the breeding of the mouse strains.

References

Ando S, Tanaka Y, Waki H, Kon K, Iwamoto M, Fukui F (1998) Gangliosides and sialylcholesterol as modulators of synaptic functions. Ann N Y Acad Sci 845:232-239.

Ang CW, Jacobs BC, Laman JD (2004) The Guillain-Barre syndrome: a true case of molecular mimicry. Trends Immunol 25:61-66.

Buchwald B, Weishaupt A, Toyka KV, Dudel J (1995) Immunoglobulin G from a patient with Miller-Fisher syndrome rapidly and reversibly depresses evoked quantal release at the neuromuscular junction of mice. Neurosci Lett 201:163-166.

Bullens RW, O'Hanlon GM, Wagner E, Molenaar PC, Furukawa K, Furukawa K, Plomp JJ, Willison HJ (2002) Complex gangliosides at the neuromuscular junction are membrane receptors for autoantibodies and botulinum neurotoxin but redundant for normal synaptic function. J Neurosci 22:6876-6884.

Chamberlain LH, Burgoyne RD, Gould GW (2001) SNARE proteins are highly enriched in lipid rafts in PC12 cells: implications for the spatial control of exocytosis. Proc Natl Acad Sci U S A 98:5619-5624.

Chen YW, Pedersen JW, Wandall HH, Levery SB, Pizette S, Clausen H, Cohen SM (2007) Glycosphingolipids with extended sugar chain have specialized functions in development and behavior of Drosophila. Dev Biol 306:736-749.

Chiavegatto S, Sun J, Nelson RJ, Schnaar RL (2000) A functional role for complex gangliosides: motor deficits in GM2/GD2 synthase knockout mice. Exp Neurol 166:227-234.

Desplats PA, Denny CA, Kass KE, Gilmartin T, Head SR, Sutcliffe JG, Seyfried TN, Thomas EA (2007) Glycolipid and ganglioside metabolism imbalances in Huntington's disease. Neurobiol Dis 27:265-277.

Egorushkina NV, Ratushnyak AS, Egorushkin IV (1993) The influence of exogenous gangliosides on the dynamics of the development of prolonged posttetanic potentiation. Neurosci Behav Physiol 23:435-438.

Fishman PH (1982) Role of membrane gangliosides in the binding and action of bacterial toxins. J Membr Biol 69:85-97.

Furuse H, Waki H, Kaneko K, Fujii S, Miura M, Sasaki H, Ito KI, Kato H, Ando S (1998) Effect of the mono- and tetra-sialogangliosides, GM1 and GQ1b, on long-term potentiation in the CA1 hippocampal neurons of the guinea pig. Exp Brain Res 123:307-314.

Gong Y, Tagawa Y, Lunn MP, Laroy W, Heffer-Lauc M, Li CY, Griffin JW, Schnaar RL, Sheikh KA (2002) Localization of major gangliosides in the PNS: implications for immune neuropathies. Brain 125:2491-2506.

Green WN, Andersen OS (1991) Surface charges and ion channel function. Annu Rev Physiol 53:341-359.

Hakomori S (2003) Structure, organization, and function of glycosphingolipids in membrane. Curr Opin Hematol 10:16-24.

Halstead SK, O'Hanlon GM, Humphreys PD, Morrison DB, Morgan BP, Todd AJ, Plomp JJ, Willison HJ (2004) Anti-disialoside antibodies kill perisynaptic Schwann cells and damage motor nerve terminals via membrane attack complex in a murine model of neuropathy. Brain 127:2109-2123.

Halstead SK, Zitman FM, Humphreys PD, Greenshields K, Verschuuren JJ, Jacobs BC, Rother RP, Plomp JJ, Willison HJ (2008a) Eculizumab prevents anti-ganglioside antibody-mediated neuropathy in a murine model. Brain 131:1197-1208.

Halstead SK, Zitman FM, Humphreys PD, Greenshields K, Verschuuren JJ, Jacobs BC, Rother RP, Plomp JJ, Willison HJ (2008b) Eculizumab prevents anti-ganglioside antibody-mediated neuropathy in a murine model. Brain 131:1197-1208.

Hashiramoto A, Mizukami H, Yamashita T (2006) Ganglioside GM3 promotes cell migration by regulating MAPK and c-Fos/AP-1. Oncogene 25:3948-3955.

Inoue M, Fujii Y, Furukawa K, Okada M, Okumura K, Hayakawa T, Furukawa K, Sugiura Y (2002) Refractory skin injury in complex knock-out mice expressing only the GM3 ganglioside. J Biol Chem 277:29881-29888.

Isaev D, Isaeva E, Shatskih T, Zhao Q, Smits NC, Shworak NW, Khazipov R, Holmes GL (2007) Role of Extracellular Sialic Acid in Regulation of Neuronal and Network Excitability in the Rat Hippocampus. Journal of Neuroscience 27:11587-11594.

Kaja S, van de Ven RC, van Dijk JG, Verschuuren JJ, Arahata K, Frants RR, Ferrari MD, van den Maagdenberg AM, Plomp JJ (2007) Severely impaired neuromuscular synaptic transmission causes muscle weakness in the Cacna1a-mutant mouse rolling Nagoya. Eur J Neurosci 25:2009-2020.

Kappel T, Anken RH, Hanke W, Rahmann H (2000) Gangliosides affect membrane-channel activities dependent on ambient temperature. Cell Mol Neurobiol 20:579-590.

Kawai H, Allende ML, Wada R, Kono M, Sango K, Deng C, Miyakawa T, Crawley JN, Werth N, Bierfreund U, Sandhoff K, Proia RL (2001) Mice expressing only monosialoganglioside GM3 exhibit lethal audiogenic seizures. J Biol Chem 276:6885-6888.

Lang T, Bruns D, Wenzel D, Riedel D, Holroyd P, Thiele C, Jahn R (2001) SNAREs are concentrated in cholesterol-dependent clusters that define docking and fusion sites for exocytosis. EMBO J 20:2202-2213.

Ledeen RW (1985) Gangliosides of the neuron. Trends in Neurosciences 8:169-174.

Ledeen RW, Wu G (2006) GM1 ganglioside: another nuclear lipid that modulates nuclear calcium. GM1 potentiates the nuclear sodium-calcium exchanger. Can J Physiol Pharmacol 84:393-402.

Liu Y, Wada R, Kawai H, Sango K, Deng C, Tai T, McDonald MP, Araujo K, Crawley JN, Bierfreund U, Sandhoff K, Suzuki K, Proia RL (1999) A genetic model of substrate deprivation therapy for a glycosphingolipid storage disorder. J Clin Invest 103:497-505.

Magleby KL, Stevens CF (1972) A quantitative description of end-plate currents. J Physiol 223:173-197.

Marconi S, Acler M, Lovato L, De Toni L, Tedeschi E, Anghileri E, Romito S, Cordioli C, Bonetti B (2006) Anti-GD2-like IgM autoreactivity in multiple sclerosis patients. Mult Scler 12:302-308.

McLachlan EM, Martin AR (1980) Non-linear summation of end-plate potentials in the frog and the mouse. J Physiol 311:307-324.

Meir A, Ginsburg S, Butkevich A, Kachalsky SG, Kaiserman I, Ahdut R, Demirgoren S, Rahamimoff R (1999) Ion channels in presynaptic nerve terminals and control of transmitter release. Physiol Rev 79:1019-1088.

Nakatani Y, Kawakami K, Nagaoka T, Utsunomiya I, Tanaka K, Yoshino H, Miyatake T, Hoshi K, Taguchi K (2007) Ca channel currents inhibited by serum from select patients with Guillain-Barre syndrome. Eur Neurol 57:11-18.

Ngamukote S, Yanagisawa M, Ariga T, Ando S, Yu RK (2007) Developmental changes of glycosphingolipids and expression of glycogenes in mouse brains. J Neurochem 103:2327-2341.

O'Hanlon GM, Plomp JJ, Chakrabarti M, Morrison I, Wagner ER, Goodyear CS, Yin X, Trapp BD, Conner J, Molenaar PC, Stewart S, Rowan EG, Willison HJ (2001) Anti-GQ1b ganglioside antibodies mediate complement-dependent destruction of the motor nerve terminal. Brain 124:893-906.

Okada M, Itoh MM, Haraguchi M, Okajima T, Inoue M, Oishi H, Matsuda Y, Iwamoto T, Kawano T, Fukumoto S, Miyazaki H, Furukawa K, Aizawa S, Furukawa K (2002) b-series Ganglioside deficiency exhibits no definite changes in the neurogenesis and the sensitivity to Fas-mediated apoptosis but impairs regeneration of the lesioned hypoglossal nerve. J Biol Chem 277:1633-1636.

Ortiz N, Rosa R, Gallardo E, Illa I, Tomas J, Aubry J, Sabater M, Santafe M (2001) IgM monoclonal antibody against terminal moiety of GM2, GalNAc-GD1a and GalNAc-GM1b from a pure motor chronic demyelinating polyneuropathy patient: effects on neurotransmitter release. J Neuroimmunol 119:114-123.

Plomp JJ, Molenaar PC, O'Hanlon GM, Jacobs BC, Veitch J, Daha MR, van Doorn PA, van der Meche FG, Vincent A, Morgan BP, Willison HJ (1999) Miller Fisher anti-GQ1b antibodies: alpha-latrotoxin-like effects on motor end plates. Ann Neurol 45:189-199.

Proia RL (2003) Glycosphingolipid functions: insights from engineered mouse models. Philos Trans R Soc Lond B Biol Sci 358:879-883.

Rahmann H, Jonas U, Kappel T, Hilderbrandt H (1998) Differential involvement of gangliosides versus phospholipids in the process of temperature adaptation in vertebrates. A comparative phenomenological and physicochemical study. Ann N Y Acad Sci 845:72-91.

Ramirez OA, Gomez RA, Carrer HF (1990) Gangliosides improve synaptic transmission in dentate gyrus of hippocampal rat slices. Brain Res 506:291-293.

Roth J, Kempf A, Reuter G, Schauer R, Gehring WJ (1992) Occurrence of sialic acids in Drosophila melanogaster. Science 256:673-675.

Salaun C, James DJ, Chamberlain LH (2004) Lipid rafts and the regulation of exocytosis. Traffic 5:255-264.

Santafe MM, Sabate MM, Garcia N, Ortiz N, Lanuza MA, Tomas J (2005) Changes in the neuromuscular synapse induced by an antibody against gangliosides. Ann Neurol 57:396-407.

Sheikh KA, Sun J, Liu Y, Kawai H, Crawford TO, Proia RL, Griffin JW, Schnaar RL (1999) Mice lacking complex gangliosides develop Wallerian degeneration and myelination defects. Proc Natl Acad Sci U S A 96:7532-7537.

Simpson MA, Cross H, Proukakis C, Priestman DA, Neville DC, Reinkensmeier G, Wang H, Wiznitzer M, Gurtz K, Verganelaki A, Pryde A, Patton MA, Dwek RA, Butters TD, Platt FM, Crosby AH (2004) Infantile-onset symptomatic epilepsy syndrome caused by a homozygous loss-of-function mutation of GM3 synthase. Nat Genet 36:1225-1229.

Sohn H, Kim YS, Kim HT, Kim CH, Cho EW, Kang HY, Kim NS, Kim CH, Ryu SE, Lee JH, Ko JH (2006) Ganglioside GM3 is involved in neuronal cell death. FASEB J 20:1248-1250.

Sonnino S, Mauri L, Chigorno V, Prinetti A (2007) Gangliosides as components of lipid membrane domains. Glycobiology 17:1R-13R.

Stevens CF, Tsujimoto T (1995) Estimates for the pool size of releasable quanta at a single central synapse and for the time required to refill the pool. Proc Natl Acad Sci U S A 92:846-849.

Sugiura Y, Furukawa K, Tajima O, Mii S, Honda T, Furukawa K (2005) Sensory nerve-dominant nerve degeneration and remodeling in the mutant mice lacking complex gangliosides. Neuroscience 135:1167-1178.

Susuki K, Baba H, Tohyama K, Kanai K, Kuwabara S, Hirata K, Furukawa K, Furukawa K, Rasband MN, Yuki N (2007) Gangliosides contribute to stability of paranodal junctions and ion channel clusters in myelinated nerve fibers. Glia 55:746-757.

Svennerholm L (1994) Designation and schematic structure of gangliosides and allied glycosphingolipids. Prog Brain Res 101:XI-XIV.

Takamiya K, Yamamoto A, Furukawa K, Yamashiro S, Shin M, Okada M, Fukumoto S, Haraguchi M, Takeda N, Fujimura K, Sakae M, Kishikawa M, Shiku H, Furukawa K, Aizawa S (1996) Mice with disrupted GM2/GD2 synthase gene lack complex gangliosides but exhibit only subtle defects in their nervous system. Proc Natl Acad Sci U S A 93:10662-10667.

Tanaka Y, Waki H, Kon K, Ando S (1997) Gangliosides enhance KCl-induced Ca2+ influx and acetylcholine release in brain synaptosomes. Neuroreport 8:2203-2207.

Taverna E, Saba E, Rowe J, Francolini M, Clementi F, Rosa P (2004) Role of lipid microdomains in P/Q-type calcium channel (Cav2.1) clustering and function in presynaptic membranes. J Biol Chem 279:5127-5134.

Tettamanti G, Bonali F, Marchesini S, Zambotti V (1973) A new procedure for the extraction, purification and fractionation of brain gangliosides. Biochim Biophys Acta 296:160-170.

Varoqueaux F, Sons MS, Plomp JJ, Brose N (2005) Aberrant morphology and residual transmitter release at the Munc13-deficient mouse neuromuscular synapse. Mol Cell Biol 25:5973-5984.

Wang YL, Tsui ZC, Yang FY (1999) Antagonistic effect of ganglioside GM1 and GM3 on the activity and conformation of sarcoplasmic reticulum Ca2+-ATPase. Febs Letters 457:144-148.

Wieraszko A, Seifert W (1985) The role of monosialoganglioside GM1 in the synaptic plasticity: in vitro study on rat hippocampal slices. Brain Res 345:159-164.

Willison HJ, Yuki N (2002) Peripheral neuropathies and anti-glycolipid antibodies. Brain 125:2591-2625.

Wood SJ, Slater CR (2001) Safety factor at the neuromuscular junction. Prog Neurobiol 64:393-429.

Wu G, Lu ZH, Obukhov AG, Nowycky MC, Ledeen RW (2007) Induction of calcium influx through TRPC5 channels by cross-linking of GM1 ganglioside associated with alpha5beta1 integrin initiates neurite outgrowth. J Neurosci 27:7447-7458.

Wu G, Lu ZH, Wang J, Wang Y, Xie X, Meyenhofer MF, Ledeen RW (2005) Enhanced susceptibility to kainate-induced seizures, neuronal apoptosis, and death in mice lacking gangliotetraose gangliosides: protection with LIGA 20, a membrane-permeant analog of GM1. J Neurosci 25:11014-11022.

Wu G, Lu ZH, Xie X, Ledeen RW (2004) Susceptibility of cerebellar granule neurons from GM2/GD2 synthase-null mice to apoptosis induced by glutamate excitotoxicity and elevated KCl: rescue by GM1 and LIGA20. Glycoconj J 21:305-313.

Wu GS, Vaswani KK, Lu ZH, Ledeen RW (1990) Gangliosides stimulate calcium flux in neuro-2A cells and require exogenous calcium for neuritogenesis. J Neurochem 55:484-491.

Yamashita T, Wu YP, Sandhoff R, Werth N, Mizukami H, Ellis JM, Dupree JL, Geyer R, Sandhoff K, Proia RL (2005) Interruption of ganglioside synthesis produces central nervous system degeneration and altered axon-glial interactions. Proc Natl Acad Sci U S A 102:2725-2730.

Yates AJ, Rampersaud A (1998) Sphingolipids as receptor modulators. An overview. Ann N Y Acad Sci 845:57-71.

Figure legends

Figure 1. Synthesis of the ganglioside family

Ganglioside nomenclature is according to Svennerholm (Svennerholm, 1994). Membranes of WT mice contain all the gangliosides. GD3s-KO mice lack the GD3s gene, which results in the absence of all the gangliosides within the dashed rectangle (b- and c-series). dKO mice lack both the GalNAc-transferase and the GD3s genes, leaving expression of only GM3 and its precursor lactosylceramide (LacCer), shown within the continuous rectangle.
NeuAc: neuraminic acid (or sialic acid); GalNAc: N-acetylgalactosamine; GalNAc-T: N-acetylgalactosamine transferase; GD3s: GD3 synthase. Arrows represent the stepwise biosynthesis through glycosyltransferases.

Figure 2. In vivo assessment of neuromuscular functioning

Mouse respiration was characterized with non-invasive plethysmography (n= 8-20). **A**. Respiration frequency was ~40% higher in WT mice than in the other two groups. **B**. The positive peak of the plethysmography signal (reflecting tidal volume) was ~35% higher in dKO mice, compared to WT and GD3s-KO. **C.** Typical examples of respiration traces recorded. **D.** Grip strength was averaged for ten trials and normalized to the body weights of the mice; all groups pulled ~6 gram per gram bodyweight (n=7-20). **E.** Hanging times in the inverted screen test. A maximum hanging time of 300 s was chosen. dKO mice had considerably shorter hanging times than WT and GD3s-KO mice (n= 5-20).
*p<0.05; **p<0.01

Figure 3. Basic ACh release parameters at the NMJ

Ex vivo electrophysiological measurements at NMJs of phrenic nerve-diaphragm preparations were performed at 24-26 °C in standard Ringer's medium. Each genotype group consisted of at least 5 mice. **A**. Uniquantal size measured as MEPP amplitude. **B**. Spontaneous uniquantal ACh release measured as MEPP frequency. **C**. EPP amplitude at 0.3 Hz stimulation. **D**. Calculated quantal content of EPP at 0.3 Hz nerve stimulation. **E**. Typical examples of MEPP recordings. **F**. Typical examples of EPP recordings. No statistically significant differences between genotypes were observed.

Figure 4. Hypertonic medium-evoked ACh release

MEPP frequency in hypertonic medium (0.5 mM sucrose-Ringer's). No statistically significant differences between genotypes were observed (n=3-5).

Figure 5. Evoked ACh release at high rate stimulation frequencies

A. Mean EPP rundown profile at 40 Hz stimulation. Each EPP in the trains is expressed as percentage of the first EPP. dKO EPPs ran down more pronounced than WT and GD3s-KO EPPs ($^{\#}p<0.01$; n=11-12). **B.** Rundown level is expressed as the ratio of the mean amplitude of the plateau phase of the train (21^{st}-35^{th} EPP) and the amplitude of the first EPP and was measured at several stimulation frequencies for WT and dKO mice. dKO NMJs displayed lower rundown levels at all frequencies but 3 Hz (**$p<0.01$, n=7-12). **C.** Typical traces of EPP amplitude rundown profiles at 40 and 70 Hz stimulation for WT and dKO NMJs.

Figure 6. Temperature-dependency of ACh release parameters

Electrophysiological measurement of ACh release at diaphragm NMJs at different bath temperatures. Each genotype group consisted of 4-6 mice. **A**. MEPP amplitude at GD3s-KO NMJs was higher than at WT and dKO NMJs at 17 °C. **B**. No statistically significant differences between genotypes in spontaneous ACh release measured as MEPP frequency at all temperatures. **C.** Differences between genotypes in evoked EPP amplitude at 0.3 Hz nerve stimulation were found only at 17 and 35 °C ($^{\#\#}p<0.01$ for GD3s-KO vs. dKO and *$p<0.05$ for WT vs. GD3s-KO, respectively). **D**. The quantal content at GD3s-KO NMJs was higher than WT, only at 35 °C (*$p<0.05$). **E**. dKO mice have lower rundown levels than GD3s-KO and WT mice at >20 °C. EPP rundown level is expressed as the ratio of the mean amplitude of the plateau phase of the train (21^{st}-35^{th} EPP) and the amplitude of the first EPP at 40 Hz stimulation (* $p<0.05$; ** $p<0.01$). **F**. dKO and GD3s-KO EPP rundown level at 3 Hz stimulation did not differ from WT at all measured temperatures. Between each other they differed in this parameter at 17 and 30 °C ($^{\#}p<0.05$).

Figure 7. Ca^{2+}-dependency of ACh release parameters

Electrophysiological measurement of ACh release at diaphragm NMJs at different extracellular Ca^{2+} concentrations. Each genotype group consisted of 4-6 mice. No differences between genotypes in Ca^{2+}-dependency were found for (**A)** MEPP amplitude, (**B**) spontaneous uniquantal ACh release, measured as MEPP frequency, (**C**) evoked EPP

amplitude at 0.3 Hz nerve stimulation and (**D**) calculated quantal content of EPP at 0.3 Hz nerve stimulation. **E**. Rundown level of EPPs is expressed as the ratio of the mean amplitude of the plateau phase of the train (21^{st}-35^{th} EPP) and the amplitude of the first EPP at 40 Hz stimulation. At 2 and 5 mM Ca^{2+} concentrations we found a lower rundown level at dKO NMJs, compared to WT and GD3s-KO NMJs. **F**. Typical examples of EPP profiles at 40 Hz stimulation in 0.2 mM Ca^{2+} medium. **G**. EPP rundown level at 3 Hz stimulation shows a slight, but statistically significant, increase of the rundown at dKO NMJs at 5 mM Ca^{2+}, compared to WT and GD3s-KO. **H**. No differences between genotypes in paired-pulse (25 ms) facilitation.

** $p<0.01$

Figure 1, Zitman et al.

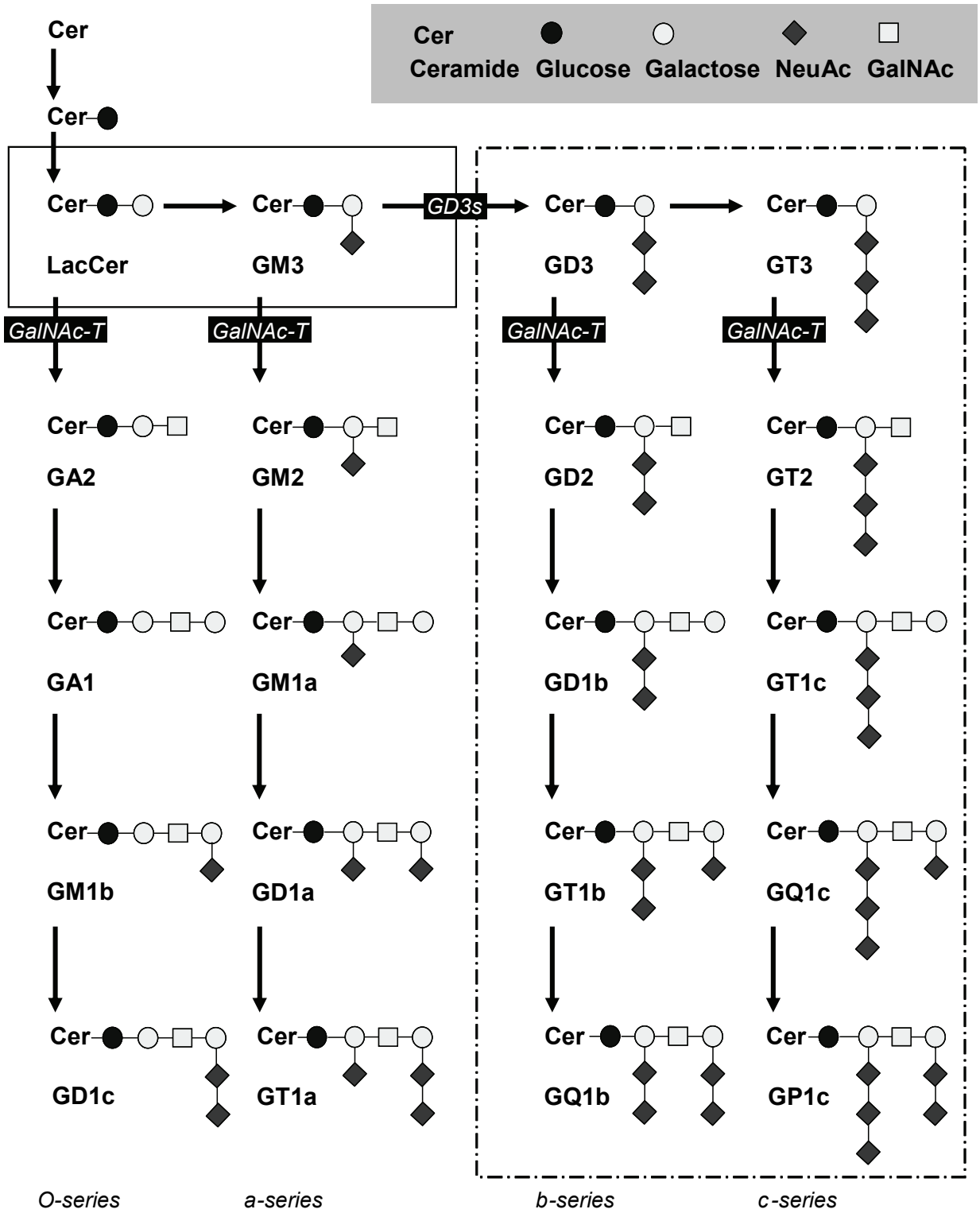

Figure 2, Zitman et al.

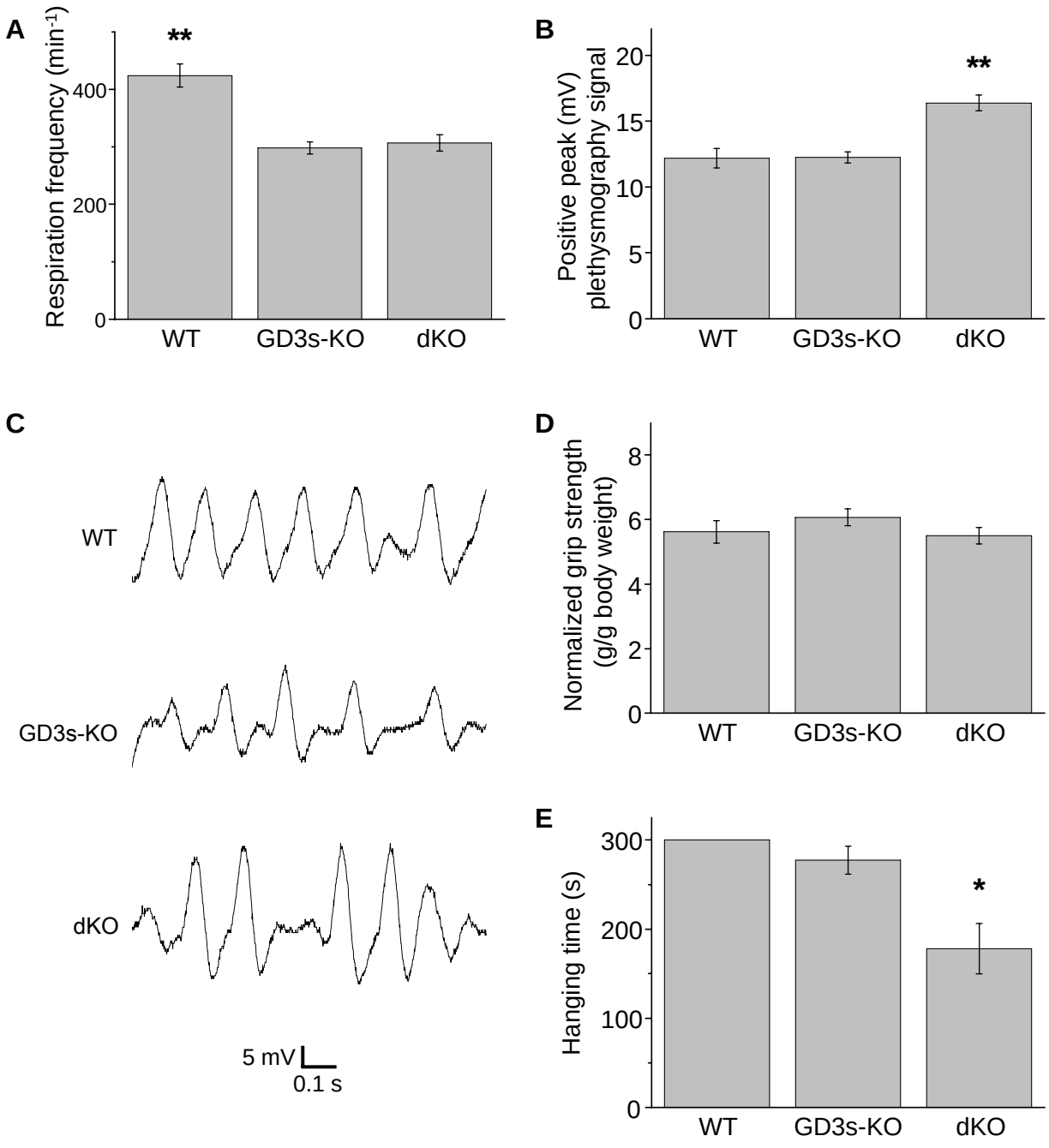

Figure 3, Zitman et al.

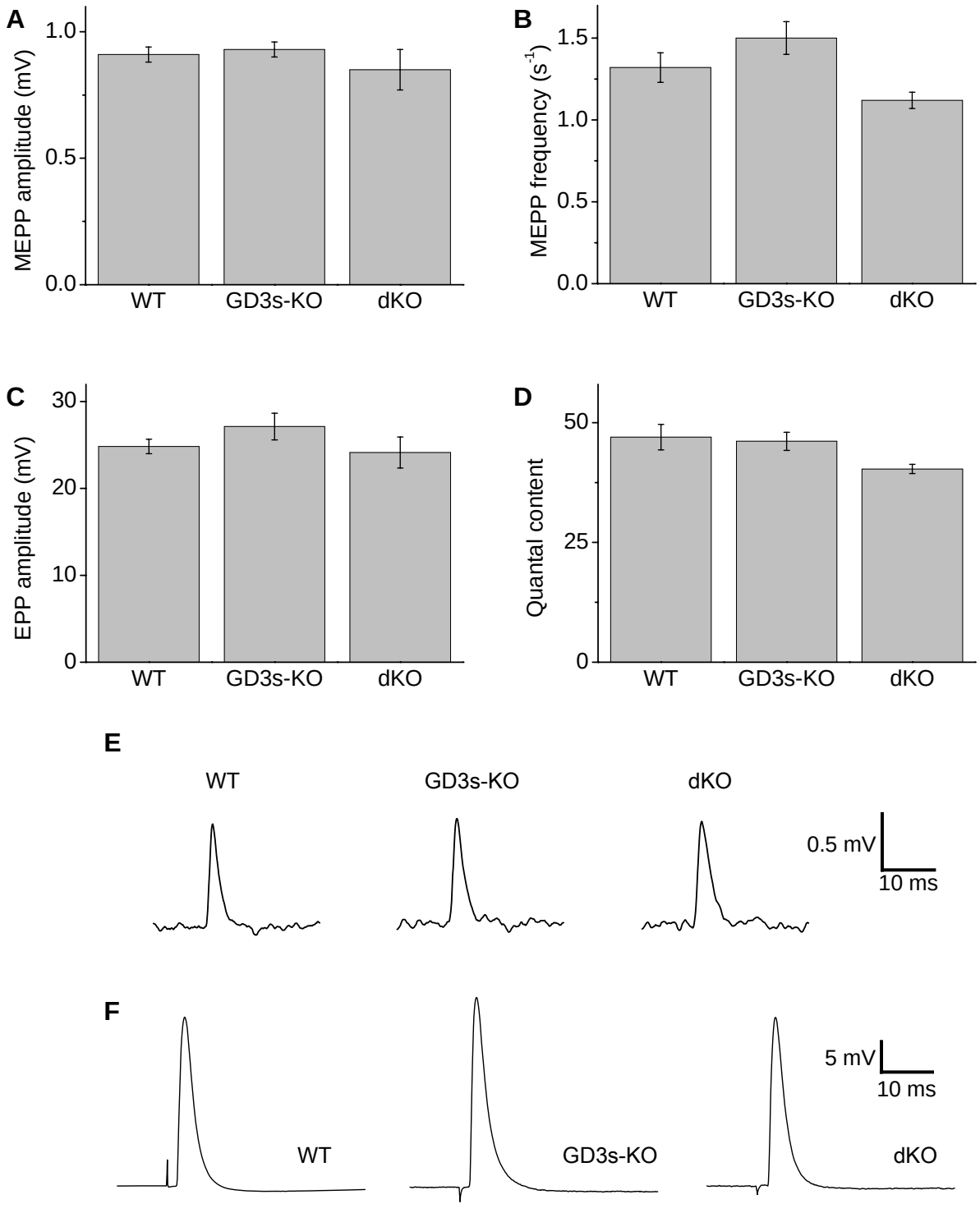

Figure 4, Zitman et al.

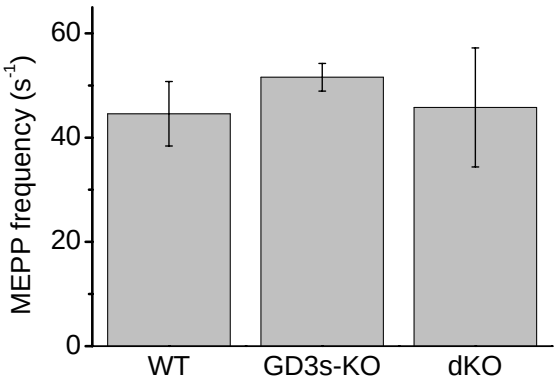

Figure 5, Zitman et al.

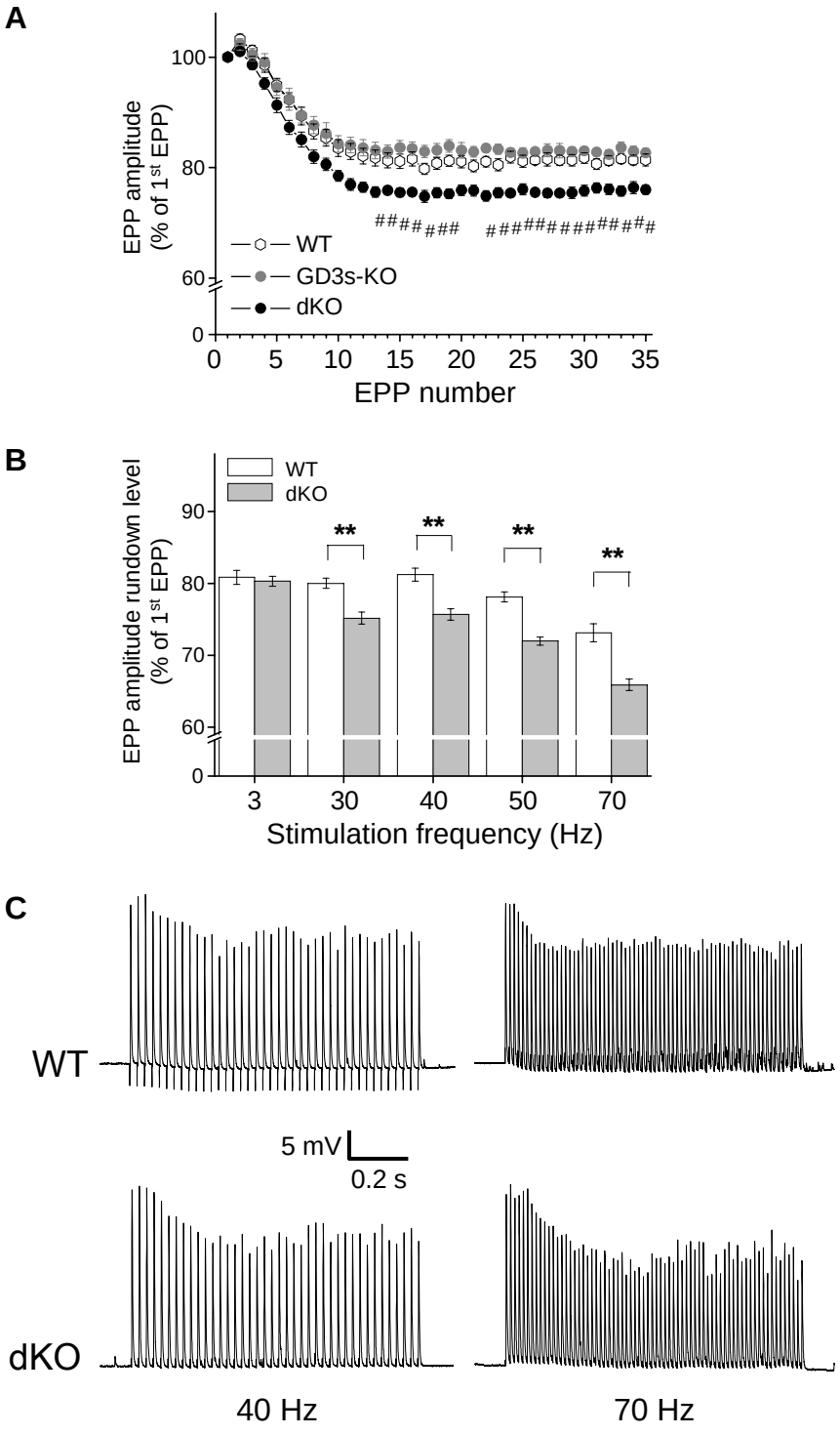

Figure 6, Zitman et al.

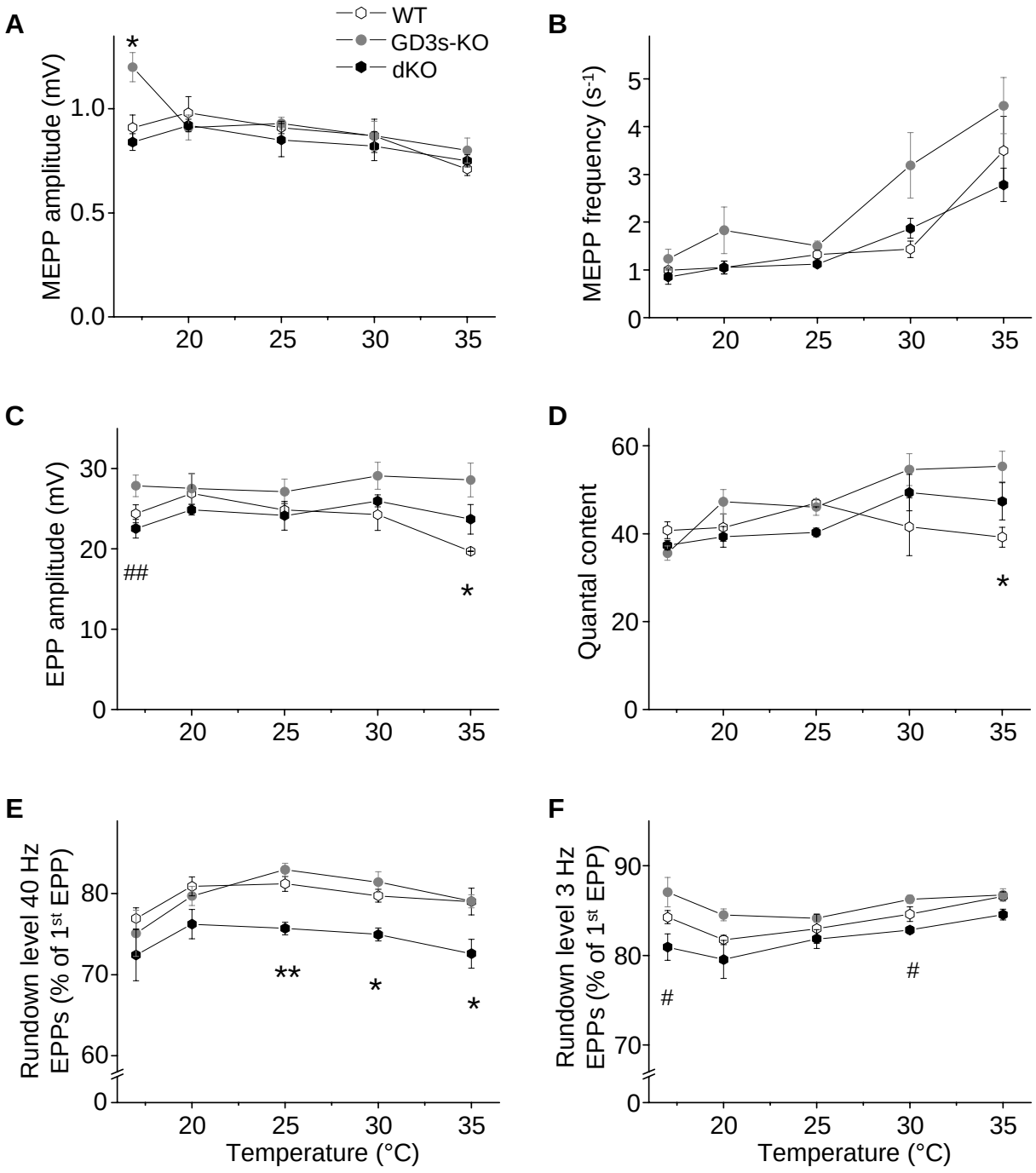

Figure 7, Zitman et al.